Available online at www.sciencedirect.com

ScienceDirect

Ceramics International 40 (2014) 2091–2095

CERAMICS INTERNATIONAL

www.elsevier.com/locate/ceramint

Synthesis as well as Raman and optical properties of Cu-doped ZnO nanorods prepared at low temperature

Javed Iqbal[a,b,*], Tariq Jan[a], M. Shafiq[c], Aqsa Arshad[a], Naeem Ahmad[a], Saeed Badshah[d], Ronghai Yu[e]

[a]*Laboratory of Nanoscience and Technology, Department of Physics, International Islamic University, H-10, Islamabad, Pakistan*
[b]*Department of Materials Science and Engineering, Tsinghua University, Beijing 100084, China*
[c]*Department of Physics, Quaid-i-Azam University, Islamabad, Pakistan*
[d]*Department of Mechanical Engineering, FET International Islamic University, H-10, Islamabad, Pakistan*
[e]*School of Materials Science and Engineering Beihang University, Beijing 100191 People's Republic of China*

Received 22 April 2013; received in revised form 24 July 2013; accepted 25 July 2013
Available online 2 August 2013

Abstract

Cu-doped ZnO nanorods have been synthesized by a low temperature, simple, fast and versatile fabrication approach. The prepared nanorods have average length and diameter of 500 nm and 40 nm, respectively. The structural and vibrational investigations depict that the prepared nanorods are in a single hexagonal phase and preferably grown along the *c*-axis. The X-rays photoelectron spectroscopy reveals that Cu is in 2+ oxidation state and doped up to 3% into the ZnO lattice. The magnetic measurements of doped nanorods show diamagnetic behavior at room temperature and paramagnetism at 8 K. The photoluminescence study shows that there is a considerable red-shift in the optical band-gap with Cu doping into ZnO and it exhibits improved luminescence properties. This tuned band-gap makes this a potential material for use in photo-catalysis, optoelectronics and solar-cell nanodevices.

Keywords: D. ZnO; Cu doping; Tailoring in band-gap; Red-shift; Nanorods

1. Introduction

Unique shape nanomaterials have attracted a lot of interest in these days because of the possibilities which they herald for a technological revolution [1]. The chemical solution based fabrication of nanomaterials is a skill for the controlled crystal growth which leads to materials not only differing in dimensions but also in shapes [2]. The crystallization is a primordial practice to obtain symmetric crystal morphology which is based on the concepts of nucleation, common ion effect, precipitation, co-precipitation and solubility product [3]. Among various shaped nanomaterials, nanorods are of special interest because of their exclusive shape-dependent applications. ZnO is one of the most potential materials for devices which requires good performance at room temperature because of its 3.37 eV direct wide band-gap with a 60 meV high exciton binding energy. Thus, ZnO nanorods have shown a great potential for many applications such as FETs, photodiodes, chemical sensors, biological sensors, light emitting diodes and solar-cells [4–8]. However, for most of the practical applications, proper dopants may be introduced into ZnO matrix in order to tune its structural, morphological, optical and magnetic properties. In recent times, Cu-ion is considered as an important dopant for ZnO nanomaterials to enhance and tune their various properties [9]. Hence, the study of various properties of Cu doped ZnO is important both for scientific reasons as well as practical applications. Several fabrication techniques have been used to synthesize doped ZnO nanorods. These techniques are MOCVD, carbothermal evaporation, VPE and PLD. However, all these methods required high temperature conditions [10,11]. Compared with these techniques, the wet chemical synthesis method is a potential alternative for successful doping during the fabrication of

---

[*] Corresponding author at: Laboratory of Nanoscience and Technology, Department of Physics, International Islamic University, H-10, Islamabad, Pakistan. Tel.: +92 51 9019713.

E-mail address: javed.saggu@iiu.edu.pk (J. Iqbal).

0272-8842/$ - see front matter © 2013 Elsevier Ltd and Techna Group S.r.l. All rights reserved.
http://dx.doi.org/10.1016/j.ceramint.2013.07.122

ZnO nanostructures. This technique provides reproducible and applicable results for the mass industrial fabrication of ZnO nanorods. In the present study, high quality undoped and Cu-doped ZnO nanostructures have been synthesized using the wet chemical method. The synthesized nanostructures were studied using structural, micro-structural, photoluminescence and magnetic techniques. The observed results are not only interesting from fundamental studies point of view but also depict the attractive application prospects.

2. Experimental procedure

The undoped ZnO and Cu-doped ZnO nanostructures were prepared via the wet chemical solvo thermal technique at low-temperature. The morphology of nanorods without using any catalyst was optimized by controlling reactant concentration, reaction time, reaction temperature and pH value. The fabrication procedure for Cu doped ZnO was similar to our previously reported work with slight variation in growth parameters [11]. Briefly, in a typical synthesis, ethanolic solution of 0.5 M NaOH (purity 99%) as a precipitating agent was gradually added dropwise into a mixture having 0.05 M $Zn(NO_3)_2 \cdot 6H_2O$ (purity 99.9%) and 0.003 M $CuCl_2 \cdot 6H_2O$ (purity 99.9%) at 0 °C under vigorous magnetic stirring. The resultant mixture solution was transferred to a Teflon lined stainless steel autoclave. This autoclave was heated at 120 °C for 36 h. After this heating treatment, the autoclave was allowed to naturally cool down to room-temperature. The precipitates were separated for washing and then centrifuged at 4000 rmp. The cleaned precipitates were dehydrated at 110 °C for 10 h to get powder samples.

3. Results and discussion

The crystal structures of undoped and Cu-doped ZnO were studied with XRD. Fig. 1 shows the XRD patterns of undoped and Cu-doped ZnO and possible phase formation of Cu dopant through this synthesis process. All the diffraction peaks for Cu-doped and undoped samples are indexed to the hexagonal wurtzite structure of ZnO. The absence of metallic Cu, CuO, or Cu_2O peaks in Cu doped ZnO pattern rules out the presence of dopant-based crystalline tiny clusters. The diffraction peaks for Cu-doped ZnO sample are slightly shifted towards the higher angles as compared to the undoped ZnO sample as depicted in the inset of Fig. 1. The peak shift is in agreement with previous studies, and supports the evidences for the successful doping into the ZnO crystal structure [12,13]. The lattice constants of doped and undoped samples have been calculated through the Rietveld refinement and are found to be a=3.2489 Å, c=5.1975 Å and a=3.2509 Å, c=5.2069 Å respectively. The decrease in lattice constants as a function Cu doping may be due to the successful substitution of Zn^{2+} (0.74 Å) ions site by smaller radii Cu^{2+} (0.57 Å) ions.

Furthermore, it is also noted that the ratio of diffraction intensity of polar plane to non-polar plane ($I_{(002)}/I_{(100)}$) is significantly increased with the Cu doping as shown in Fig. 1. A high ratio of $I_{(002)}/I_{(100)}$ with Cu doping is accompanied by a large portion of polar planes, which demonstrates that the polarization plays an important role for the growth direction of prepared nanostructures[14].

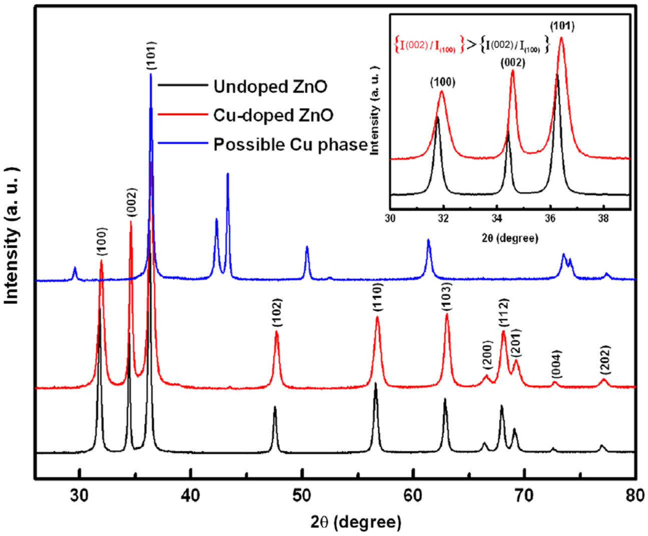

Fig. 1. XRD patterns of undoped ZnO, Cu-doped ZnO and possible Cu dopant phase.

The Cu doping induced effects on the morphology of ZnO were examined through TEM. Fig. 2(a) shows the nanorods morphology as compared to the undoped ZnO nanowires. These nanorods have a length of 300–700 nm and diameter lies in the range of 30–50 nm. They are randomly distributed over the TEM grid. The evolution of morphology from nanowires to nanorods with Cu doping is well known due to the polar structure of ZnO along the c-axis. The increase in polar planes can be understood from ratio of polar planes intensity to non-polar plane's intensity ($I_{(002)}/I_{(100)}$), as observed in XRD results. The high-resolution image (Fig. 2(b)) indicates that the growth direction of nanostructure is oriented along [0001]. The absence of visible defects, stacking fault, secondary phase or precipitation of Cu impurity in the microstructure shows that the dopant is well-incorporated into the host matrix lattice sites. The SAED pattern as shown in Fig. 2(c) is in agreement with the ZnO hexagonal wurtzite structure. The absence of any extra phase of Cu dopant in SAED pattern further confirms the XRD results. Consequently, it can be concluded that Cu dopant is incorporated into the host lattice structure without any distortion in the crystallinity.

The contents and oxidation state of Cu cations into ZnO were investigated using XPS technique and the spectrum is shown in Fig. 3. The peaks position of Cu $2p_{3/2}$ and Cu $2p_{1/2}$ splitting components of Cu $2p$ in the XPS spectrum are centered on 932.9 ± 0.10 eV and 912.3 ± 0.10 eV, respectively. The shape, presence of satellite lines, and difference of binding energy between these two components clearly show that Cu is in 2+ oxidation state in the ZnO lattice. Furthermore, the XPS sample surface study reveals that Cu is about ~3% doped into the host lattice and its value is shown in Table 1.

Fig. 4 depicts the room-temperature Raman spectrum of the as prepared Cu-doped ZnO nanorods. It is reported in the

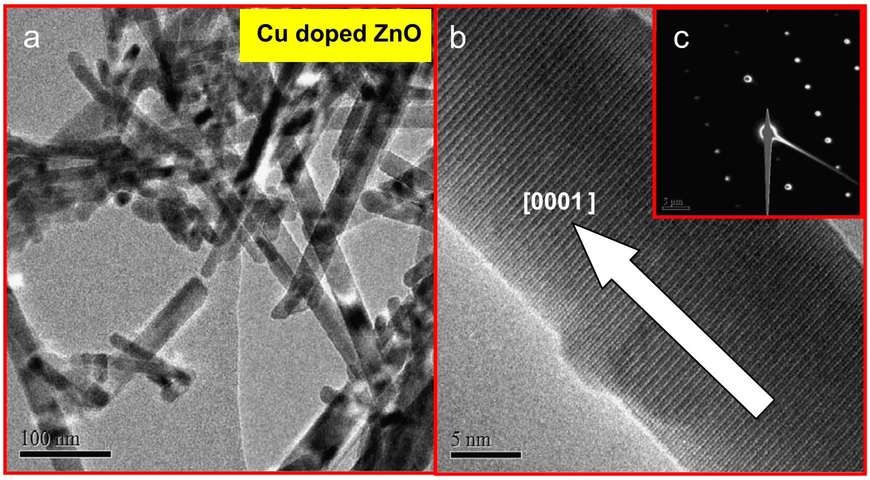

Fig. 2. (a) TEM, (b) HRTEM and (c) SAED pattern of Cu-doped ZnO nanorods.

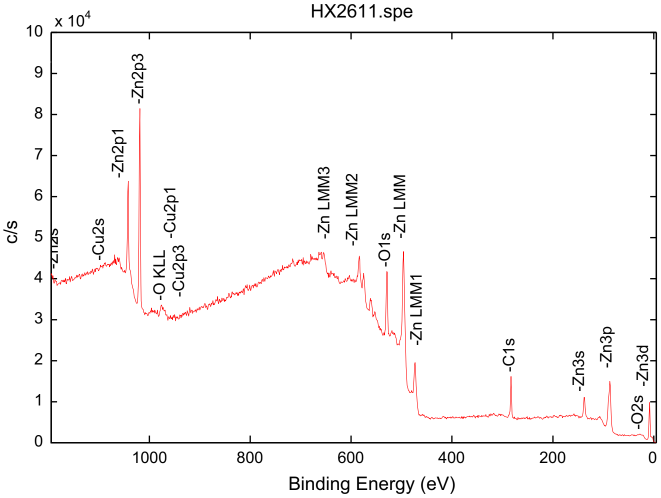

Fig. 3. XPS spectrum of Cu-doped ZnO nanorods.

Table 1
Atomic concentration.

C 1*s*	O 1*s*	Cu $2p^3$	Zn $2p^3$
[0.314] 43.06	[0.733] 40.04	[2.626] 0.03	[2.768] 16.86

standard zone-center optical phonon frequencies spectrum of ZnO [15] that the vibrational mode at 319 cm^{-1} corresponds to the 2nd order Raman spectrum which arises due to the zone boundary phonons (E_{2H}–E_{2L}). The peak at 426 cm^{-1} should be assigned to ZnO non-polar high-frequency E_{2H} mode. This mode represents the band characteristic of hexagonal wurtzite phase [16]. The Raman peak at 565 cm^{-1} belongs to E_1(LO) mode and has a significant red-shift from wurtzite characteristic vibrational mode (580 cm^{-1}). This shift clearly depicts that there are a large number of defects (i.e. zinc interstitial and oxygen vacancy defect states) present in ZnO nanorods. The absence of extra vibrational mode corresponding to some secondary phase confirms the successful doping of Cu into the hexagonal wurtzite structure of ZnO nanostructures. These results are consistent with the studies of XRD, HRTEM and SAED investigations.

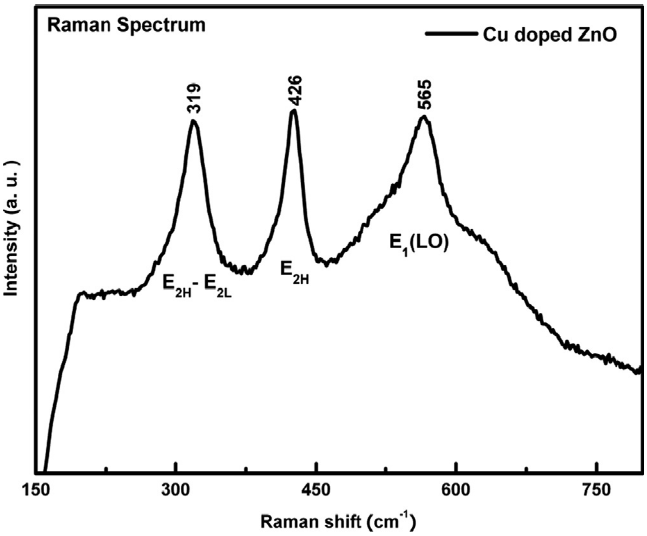

Fig. 4. Raman spectrum of Cu-doped ZnO nanorods.

Photoluminescence (PL) study is an important way to understand the electronic band structure and optical properties of semiconductor nanostructures. Using this technique, information about band-gap, oxygen vacancy defects, separation and recombination of photo-induced charge carriers can be acquired. Room temperature PL spectrum of prepared samples has been obtained using He–Cd laser having a lasing wavelength of 325 nm as an excitation source. Fig. 5 depicts the PL spectra of undoped and Cu-doped ZnO nanostructures. There are two different emission peaks found in each spectrum. The sharp transition peak with high intensity lies in the UV region while another broad emission is found in the visible green region. The UV peak is related to direct band-gap of zinc oxide and the green emission peak is mostly attributed to the defects arising from the singly ionized oxygen vacancies or Zn interstitial [17].

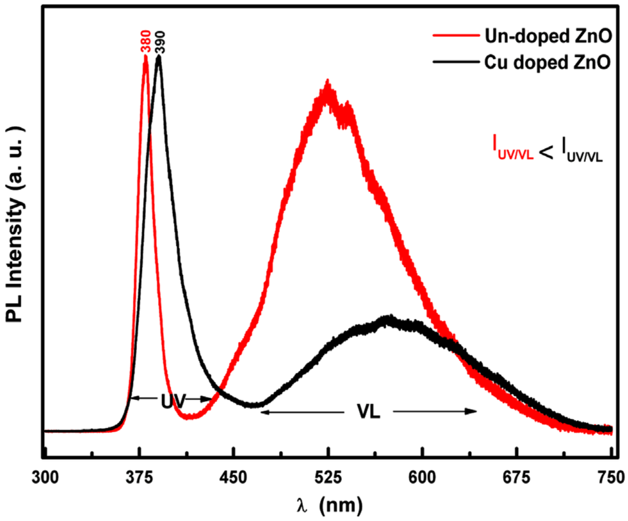

Fig. 5. Room temperature PL spectra of undoped and Cu-doped ZnO nanomaterials.

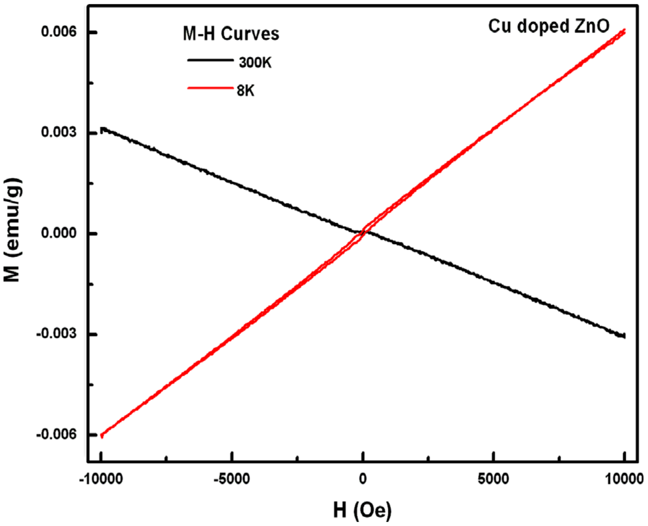

Fig. 6. *M–H* curves of Cu-doped ZnO at 300 K and 8 K.

The UV transition peaks of undoped and Cu doped ZnO nanostructures are located at 380 nm and 390 nm, respectively. The red-shift of ~10 nm in Cu-doped ZnO nanorods shows an obvious decrease in the band-gap of ZnO as a function of the Cu dopant. This tailoring in band-gap with Cu doping also depicts that the dopant ions have been successfully substituted for the Zn lattice ions sites into the ZnO host lattice [18]. It is also interestingly found that the intensity ratio of UV to visible peak ($I_{UV/VL}$) for Cu-doped ZnO nanorods is higher than that of undoped ZnO nanowires, which shows an improvement in the crystal band and luminescence property.

Recently, many researchers reported about room temperature ferromagnetism of Cu doped ZnO nanostructures [19]. This ferromagnetism is mostly attributed to the crystal structure defect. In order to know about the magnetic behavior of as prepared Cu doped ZnO nanorods, *M–H* loops were measured at 8 K and room-temperature. The *M–H* curves in Fig. 6 show that Cu-doped ZnO nanorods demonstrate diamagnetic behavior at room temperature and paramagnetism at low temperature.

The highly reported ferromagnetism in Cu doped ZnO was observed for the mixed or Cu^+ oxidation state. The electronic configuration of outer shell of Cu atoms in the ground state is $3d^{10}4s^1$, while Cu^+ and Cu^{2+} ions have $3d^{10}$ and $3d^9$ electronic configurations, respectively. The uncompensated spin of electron in $3d^9$ configuration of Cu^{2+} ions with 1/2 spin angular momentum gives rise to a net magnetic moment of 1 μ_B [20]. As found from the XPS spectrum the Cu ions are in 2+ oxidation states but do not contribute to the activation of ferromagnetism in prepared Cu-doped ZnO nanorods due to the presence of defects which randomize their moments.

4. Conclusions

In summary, high quality Cu-doped ZnO nanorods were successfully fabricated by a versatile, catalyst free and reproducible wet chemical technique. Structural characterization reveals that Cu ions are successfully incorporated into the ZnO lattice without any extra phase and wurtzite structure of ZnO is retained. The average length and diameter of nanorods are 500 nm and 40 nm, respectively. It has been observed that Cu is in 2+ oxidation state and is doped up to 3% into the ZnO lattice. The Cu doping significantly reduced the band-gap of ZnO nanorods and enhanced their luminescence properties. The magnetic measurements of doped nanowires showed diamagnetic behavior at room temperature but paramagnetic behavior at 8 K.

Acknowledgments

This work was funded by the HEC Project IPFP (Grant No. No: PM-IPFP/HRD/HEC/2011/3386), HEC Ph.D. Scholar funding and PSF Project C-QU/phys. (136).

References

[1] C.N. Rao, A. Muller, A.K. Cheetham, in: Nanomaterials Chemistry: Recent Developments and New Directions, John Wiley, Hoboken, NJ, 2007.
[2] L. Li, N. Koshizaki, G.H. Li, Nanotube arrays in porous anodic alumina membranes, Journal of Materials Sciences and Technology 24 (2008) 550–562.
[3] J.W. Mullin, in: Crystallization, 4th edition, Butterworth-Heinemann, Oxford, UK, 2001.
[4] Y. Cui, Q.Q. Wei, H.K. Park, C.M. Lieber, Nanowire nanosensors for highly sensitive and selective detection of biological and chemical species, Science 293 (2001) 1289–1292.
[5] M. Law, L.E. Greene, J.C. Johnson, R. Saykally, P. Yang, Nanowire dye-sensitized solar cells, Nature Materials 4 (2005) 455–459.
[6] M.S. Arnold, P. Avouris, Z.W. Pan, Z.L. Wang, Field-effect transistors based on single semiconducting oxide nanobelts, Journal of Physical Chemistry B 107 (2003) 659–663.
[7] M.C. Jeong, B.Y. Oh, M.H. Ham, S.W. Lee, J.M. Myoung, ZnO-nanowire-inserted GaN/ZnO heterojunction light-emitting diodes, Small 3 (2007) 568–572.

[8] H. Zhou, G.J. Fang, L.Y. Yuan, C. Wang, X.X. Yang, H.H. Huang, C.H. Zhou, X.Z. Zhao, Deep ultraviolet and near infrared photodiode based on n-ZnO/p-silicon nanowire heterojunction at low temperature, Applied Physics Letters 94 (2009) 013503.

[9] S. Singhal, J. Kaur, T. Namgyal, R. Sharma, Cu-doped ZnO nanoparticles: synthesis, structural and electrical properties, Physica B 407 (2012) 1223–1226.

[10] J. Sin, S. Lam, K. Lee, A.R. Mohamed, Preparation and photocatalytic properties of visible light-driven samarium-doped ZnO nanorods, Ceramics International 39 (2013) 5833–5843.

[11] J. Iqbal, B. Wang, X. Liu, D. Yu, B. He, R. Yu, Oxygen-vacancy-induced green emission and room-temperature ferromagnetism in Ni-doped ZnO nanorods, New Journal of Physics 11 (2009) 01–14.

[12] G. Srinet, R. Kumar, V. Sajal, Effects of Ni doping on structural, optical and dielectric properties of ZnO, Ceramics International 39 (2013) 7557–7561.

[13] T.S. Herng, S.P. Lau, S.F. Yu, et al., Magnetic anisotropy in the ferromagnetic Cu-doped ZnO nanoneedles, Applied Physics Letters 90 (2007) 032509.

[14] G.R. Li, T. Hu, G.L. Pan, T.Y. Yan, X.P. Gao, H.Y. Zhu, Morphology function relationship of ZnO: polar planes, oxygen vacancies and activity, Journal of Physical Chemistry C 112 (2008) 11859–11864.

[15] C.A. Arguello, D.L. Rousseau, S.P. Porto, First-order Raman effect in wurtzite-type crystals, Physical Review 181 (1969) 1351–1363.

[16] J. Serrano, A.H. Romero, F.J. Manjon, et al., Pressure dependence of the lattice dynamics of ZnO: an ab initio approach, Physical Review B 69 (2004) 094306–094314.

[17] N.Y. Garces, L. Wang, L. Bai, N.C. Giles, L.E. Halliburton, G. Cantwell, Role of copper in the green luminescence from ZnO crystals, Applied Physics Letters 81 (2002) 622–624.

[18] C.X. Xu, X.W. Sun, X.H. Zhang, L. Ke, S.J. Chua, Photoluminescent properties of copper-doped zinc oxide nanowires, Nanotechnology 15 (2004) 856–861.

[19] Guodong Tang, Xiaoqin Shia, Chao Huo, Zhihe Wang, Room temperature ferromagnetism in hydrothermally grown Ni and Cu co-doped ZnO nanorods, Ceramics International 39 (2013) 4825–4829.

[20] Gaurav Shukla, Magnetic and optical properties of epitaxial n-type Cu-doped ZnO thin films deposited on sapphire substrates, Applied Physics A 97 (2009) 115–118.